NMR Spectroscopy

International Edition: DOI: 10.1002/anie.201908416
German Edition: DOI: 10.1002/ange.201908416

Observation and Kinetic Characterization of Transient Schiff Base Intermediates by CEST NMR Spectroscopy

Venkatraman Ramanujam[+], Cyril Charlier[+], and Ad Bax**

Abstract: *In aqueous solution, many biochemical reaction pathways involve reaction of an aldehyde with an amine, which progresses through generally unstable, hydrated and dehydrated, Schiff base intermediates that often are unobservable by conventional NMR. There are 4 states in the relevant equilibrium: 1) gem-diol, 2) aldehyde, 3) hemiaminal, and 4) Schiff base. For the reaction between protein amino groups and DOPAL, a highly toxic metabolite of dopamine, the ^{1}H resonances of both the hemiaminal and the dehydrated Schiff base can be observed by CEST NMR, even when their populations fall below 0.1 %. CEST NMR reveals the quantitative exchange kinetics between reactants and Schiff base intermediates, explaining why the Schiff base NMR signals are rarely observed. The reactivity of DOPAL with N$^\alpha$-amino groups is greater than with lysine N$^\varepsilon$-amines and, in the presence of O_2, both types of Schiff base DOPAL–peptide intermediates rapidly react with free DOPAL to irreversibly form dicatechol pyrrole adducts.*

As reported by Hugo Schiff in 1864,[1] nucleophilic attack on a carbonyl carbon atom by an amine can lead to a metastable hemiaminal (also known as carbinolamine) intermediate, whose subsequent dehydration generates a Schiff base (Figure 1 A). Schiff base formation is reversible, and the excess water present in physiological conditions can skew the equilibrium towards the starting materials due to the dehydration nature of the reaction. Therefore, their presence and biological importance is commonly established by cyanoborohydride reduction to stable amines. The transient nature of a Schiff base intermediate makes this structure commonly not directly observable by ^{1}H NMR spectroscopy, unless stabilized by intramolecular hydrogen bonding or locked in by covalent ring formation.[2,3]

We previously showed that the primary, highly toxic dopamine metabolite, 3,4-dihydroxyphenylacetaldehyde or DOPAL, reacts with lysine sidechain amino groups to form dicatechol pyrrole lysine (DCPL) adducts,[4] that can further react to form covalent intermolecular isoindole linkages.[5] This pathway is at the core of the "catechol-aldehyde hypothesis", which provides a plausible link between DOPAL and the presence of α-synuclein-containing aggregates in dopaminergic neurons of Parkinson's disease patients.[6–9] The first step in the reaction pathway of the DCPL adduct formation involves a Schiff base linkage between the DOPAL aldehyde and the Lys ε-amino group.[9–12] Mass spectrometry confirmed the presence of DOPAL Schiff base adducts, but typically involved trapping by cyanoborohydride, and made it difficult to assess their populations and lifetimes under physiological conditions.[4,11,12] No direct NMR evidence has been reported for Schiff base DOPAL–lysine reaction intermediates. The absence of a ^{1}H NMR signal for the Schiff base intermediate could result from its low population, or from line broadening caused by a chemical exchange process, for example, between the hydrated and dehydrated Schiff base, on a micro- to millisecond timescale. Here, we set out to resolve the causes for the absence of the Schiff base ^{1}H signals in conventional NMR spectra and show that they can be characterized quantitatively by chemical-exchange-saturation-transfer (CEST) NMR.

CEST NMR has been used extensively to characterize low populations of sparsely populated excited states in proteins in dynamic equilibrium with their major ground state,[13–15] and recently was shown to also be particularly powerful for

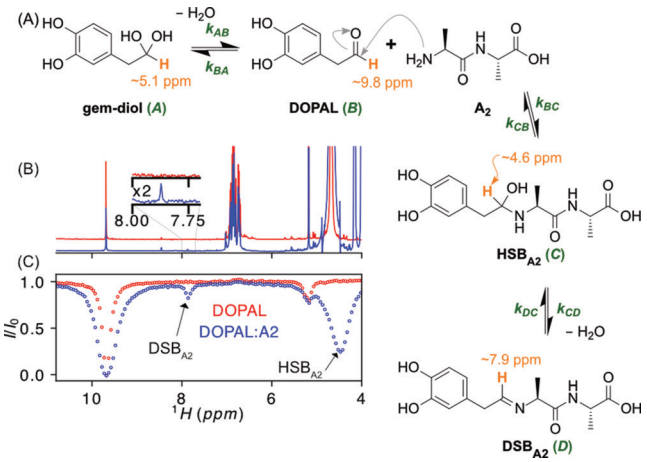

Figure 1. Formation of DOPAL–dialanine Schiff base adduct. A) Reaction Scheme. The ^{1}H used as a reporter for the four states is shown in orange. B) Superimposed ^{1}H NMR spectra of 2 mM DOPAL in the absence (red) and presence (blue) of 10 mM A_2 measured at 600 MHz, in 10 mM sodium phosphate D_2O buffer, pD 7.9, and $T = 35$ °C. C) CEST attenuation profiles of the DOPAL aldehyde signal, obtained using $B_1 = 30$ Hz, $\tau_{cest} = 5$ s, on the samples with (blue) and without (red) A_2, stepping the CEST frequency in 30 Hz increments from 4 to 11 ppm. Intensity dips assigned to the hydrated (carbinolamine) and dehydrated Schiff base positions are marked with HSB_{A2} and DSB_{A2}, respectively.

[*] Dr. V. Ramanujam,[+] Dr. C. Charlier,[+] Dr. A. Bax
Laboratory of Chemical Physics,
National Institute of Diabetes and Digestive and Kidney Diseases
Bethesda, MD 20892 (USA)
E-mail: cyril.charlier@nih.gov
bax@nih.gov

[+] These authors contributed equally to this work.

Supporting information and the ORCID identification number(s) for the author(s) of this article can be found under: https://doi.org/10.1002/anie.201908416.

identifying elusive reaction intermediates in organocatalysis, as well as for identifying predicted but previously unobserved species in silicon hydride anion clusters.[16,17] CEST is based on the original saturation transfer experiments by Forsén and Hoffman[18] and the method is widely used to encode chemical information in magnetic resonance imaging (MRI).[19,20] CEST NMR is carried out by systematically stepping the frequency of a probing radiofrequency (RF) field. We show that, once such measurements have identified the location of a hidden resonance, additionally stepping the amplitude and duration of the RF field at such a position makes quantitative analysis of the kinetic process highly robust.

In this study, we report the NMR observation of the carbinolamine and Schiff base ^{1}H resonances in the reaction between DOPAL and both the N-acetyl-Lys sidechain ε-amine as well as the N-terminal α-amine of dialanine (A_2). Anaerobic conditions were used to prevent progression of the reaction to form dicatechol pyrrole products. Populations of, in particular, the Lys C^{ε} Schiff base adduct relative to the summed populations of the dynamic equilibrium between DOPAL in its aldehyde and hydrated, gem-diol (short for geminal diol) forms remains very low (< 0.1 %) under physiological pH and temperature conditions. Higher population of the C^{α} amine Schiff base adduct (approximately 1 %) is consistent with its prior observation by mass spectrometry.[11,21] Varying the RF field strength and duration of the CEST irradiation provides direct access to the forward and reverse reaction rates, thereby yielding Arrhenius activation energies from measurement of their temperature dependencies.

CEST-based NMR analysis of Schiff base intermediates is investigated for the reaction of DOPAL with two model systems: the dipeptide L-alanyl-L-alanine (A_2), and N^{α}-acetylated lysine (AcL) as a mimic for the 15 nucleophilic lysine residues in α-synuclein. As the α-methylene protons of DOPAL slowly exchange with deuterons of the D_2O solvent, and to suppress differential J-coupling and relaxation behavior, they were fully exchanged (overnight incubation) with deuterium prior to all measurements. We first focus on the DOPAL–A_2 reaction. The DOPAL aldehyde is in equilibrium with its hydrated, gem-diol form, and the equilibrium then involves four states (Figure 1 A): the gem-diol, DOPAL, the hydrated Schiff base (HSB_{A2}) formed upon reaction of DOPAL with A_2, and the dehydrated Schiff base (DSB_{A2}).

With k_{AB} and k_{BA} not impacted by the presence of A_2, we first characterize the equilibrium between the aldehyde and gem-diol forms of DOPAL (Figure 1 A) by ^{1}H-CEST. Typically, CEST is carried out by recording a set of NMR spectra while stepwise changing the frequency of a weak, saturating RF-field of strength B_1 (applied for a duration τ_{cest}) across a region where the low-intensity peak of the minor state is expected to resonate. Chemical exchange between major and minor states during the irradiation period then will attenuate the intensity of the major site if the frequency of the CEST RF-field falls sufficiently close to that of the minor species to saturate its z magnetization. The method is equally applicable when directly observing the minor state, as applies for observation of the DOPAL aldehyde proton, which exists in a 32:68 equilibrium with its gem-diol form (5.17 ppm; Figure 1 B). The width and amplitude of the aldehyde intensity dip, observed when the RF field is applied in the vicinity of the gem-diol resonance (red trace in Figure 1 C), allows extraction of the forward and reverse rates of exchange, and of the chemical shifts.[13] As we show here, if the chemical shifts are known a priori, a robust and fast method to obtain populations and rates fixes the CEST RF frequency at that of the minor species, while stepwise varying B_1 or τ_{cest}. For CEST studies of small molecules, which can have very long T_1 relaxation times under O_2-free conditions, this can become particularly important.

With the saturating field fixed at the gem-diol resonance, attenuation of the aldehyde as a function of τ_{cest} (Supporting Information, Figure S1) is analyzed by fitting observed intensities to the Bloch–McConnell equations for a system of a single spin exchanging between two states (A: gem-diol; B: aldehyde). With the populations, p_A and p_B accurately known at each temperature from integration of their resonances in the 1D NMR spectrum, the exchange rate (k_{ex}) is then the only adjustable parameter (see the Supporting Information). The individual rate constants for the gem-diol equilibrium are derived from k_{ex}, using $k_{AB} = p_B k_{ex}$, $k_{BA} = p_A k_{ex}$ (Supporting Information, Figure S1). Measurements at temperatures, T, ranging from 20 to 45 °C then yield the activation energies (E_A^{AB}, E_A^{BA}) from the Arrhenius equation [Eq. (1)]:

$$k(T) = A\exp(-E_A/RT) \quad (1)$$

where $k(T)$ is the corresponding rate (k_{AB} or k_{BA}), A is the fitted pre-exponential factor, and R is the universal gas constant. Activation energies are $E_A^{AB} = 18.7 \pm 0.2$ kcal mol^{-1} and $E_A^{BA} = 11.9 \pm 0.1$ kcal mol^{-1} for the forward and reverse directions, respectively.

Next, we investigate Schiff base formation between DOPAL and A_2 (Figure 1 A) for a sample containing 2 mM DOPAL and 10 mM A_2. A very weak resonance assigned to the Schiff base (DSB_{A2}) is present in the ^{1}H NMR spectrum (blue inset, Figure 1 B, and Supporting Information, Figure S2), but the HSB_{A2} resonance is not observed (Figure 1 B and Supporting Information, Figure S2). This latter resonance is revealed by the ^{1}H-CEST profile, which shows a deep, broad intensity dip slightly upfield of the residual HDO frequency (Figure 1 C and Supporting Information, Figure S2 B). To investigate the kinetics, ^{1}H-CEST data were recorded with the saturation B_1 field applied at the now known HSB_{A2} and DSB_{A2} frequencies, while observing the intensity of the aldehyde resonance (Figure 2). Saturation profiles are shown as a function of saturation time (0.1 s–5 s; Figure 2 A,B), B_1 RF field strength (3 Hz–100 Hz; Figure 2 C,D) and offset around the HSB_{A2} resonance frequency (Figure 2 E), followed by analysis using a four-state-exchange Bloch–McConnell equation (Supporting Information, Eq. S5) to describe the reaction scheme of Figure 1 A. Details of the fitting procedure are presented in the Supporting Information.

With the gem-diol/aldehyde interconversion rates known from the above measurements on free DOPAL, the direct observation of the DSB_{A2} resonance (blue spectrum in Figure 1 B) allows us to fix the ratio $p_D/p_B \approx 4$ % at all temperatures. For the fitting procedure, the resonance frequencies of the gem-diol, aldehyde, and DSB_{A2} proton

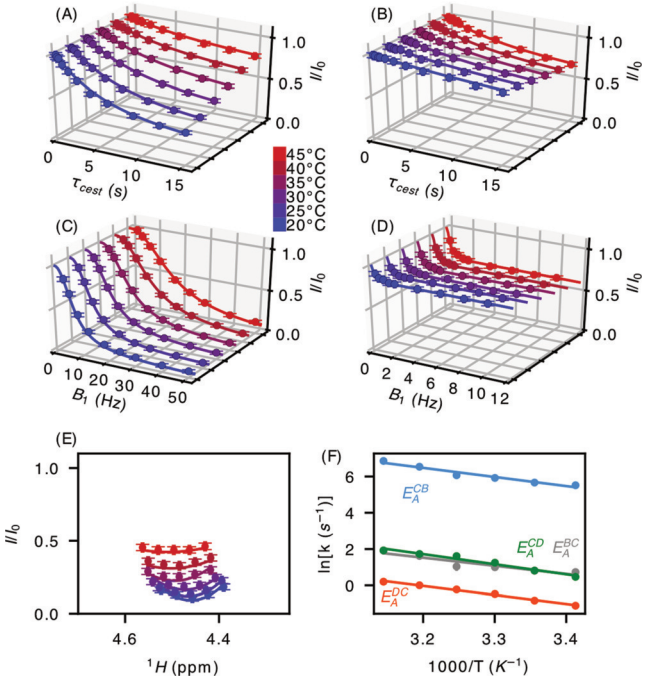

Figure 2. Schiff base formation between DOPAL and dialanine. Saturation profiles of the aldehyde resonance in the presence of 10 mM A_2 upon irradiation of the hydrated (A,C) and dehydrated (B,D) Schiff base resonance for temperatures ranging from 20 to 45 °C. (A,B) were recorded with $B_1 = 10$ Hz and τ_{cest} ranging from 0.1 to 15 s. (C,D) were recorded with $\tau_{cest} = 30$ s and B_1 from 3 to 100 Hz. (E) was recorded with $B_1 = 30$ Hz and $\tau_{cest} = 5$ s, for 5 offset frequencies around the HSB_{A2} resonance. F) Activation energies calculated for the DOPAL/Schiff base reaction ($E_A^{BC} = 8.8 \pm 1.6$ kcal mol^{-1} and $E_A^{CB} = 10.0 \pm 1.1$ kcal mol^{-1}) and the hemiaminal/Schiff base reaction ($E_A^{CD} = 11.0 \pm 0.9$ kcal mol^{-1} and $E_A^{DC} = 9.8 \pm 0.4$ kcal mol^{-1}).

were obtained from the regular 1D NMR spectrum, while the chemical shift of HSB_{A2} at each temperature was rapidly and precisely determined using the ^{1}H-CEST approach, applied over a very limited range of frequencies around the approximately known position (Supporting Information, Figure S2B). Subsequently, only three variables (k_{BC}, k_{CB}, k_{CD}) require fitting at each temperature (Supporting Information, Figure S3) and their temperature dependence yields the activation energies (Figure 2F).

The reaction scheme in Figure 1A applies to the solution of DOPAL and dialanine under anaerobic conditions. If no special precautions are taken to remove O_2, the Schiff base adduct will react with free DOPAL to form a relatively stable dicatechol pyrrole dialanine (DCPdA) product (Supporting Information, Figure S4). Formation of its pyrrole ring presumably involves oxidization steps and intermediates similar to those in the Paal–Knorr mechanism,[22,23] fully analogous to formation of dicatechol pyrrole lysine, reported previously.[4] Mass spectrometry and HMBC NMR data collected in deuterated methanol, where DCPdA is stable for days, were used to validate its structure (Supporting Information, Figures S5 and S6).

Next, we used CEST NMR to investigate the reaction with lysine ε-amino groups, using N^{α}-acetylated lysine (AcL) as a mimic for the 15 Lys residues in α-synuclein, whose reaction with DOPAL has been implicated in Parkinson's disease.[6–9] (Figure 3A). In contrast to the DOPAL reaction with A_2, neither the Schiff base nor its hydrated hemiaminal form (DSB_{AcL} and HSB_{AcL}, respectively) are directly observable in the DOPAL:AcL NMR spectrum (Figure 3B). However, the HSB_{AcL} yields a strong ^{1}H-CEST signal at 20 °C, slightly upfield but partly overlapping with the gem-diol ^{1}H resonance (Figure 3C). The effect of saturating the DSB_{AcL} resonance at 7.82 ppm was also observed by ^{1}H-CEST but was much weaker and only visible above room temperature. These ^{1}H-CEST data were recorded with a weaker saturating field of 6 Hz to minimize direct saturation of the aldehyde resonance, and narrower frequency windows centered around the resonance frequency of each state were used after a preliminary coarser CEST scan of the full spectrum. Such profiles were recorded with 30 Hz RF field and $\tau_{CEST} = 5$ s (HSB_{AcL}) and 6 Hz RF field and $\tau_{CEST} = 15$ s (DSB_{AcL}) to identify the approximate positions. The HSB_{AcL} CEST signal progressively broadens with temperature and was no longer observable above 35 °C (Supporting Information, Figure S7C). With δHSB_{AcL} and δDSB_{AcL} known, measurement of the ^{1}H CEST effect as a function of B_1 and τ_{cest} was used to obtain quantitative rates (Supporting Information, Figure S7). Analysis again involved a four-state exchange system, with state A the gem-diol, B the directly observed aldehyde, C the HSB_{AcL} and D the DSB_{AcL}. In contrast to the DOPAL–A_2 reaction, the ratio p_B/p_D could not be determined by inspection of the conventional ^{1}H NMR spectrum, therefore requiring fitting of four exchange rates: k_{BC}, k_{CB}, k_{CD}, and k_{DC} (Figure 3), with results summarized in Table S2 in the Supporting Information.

Equilibrium populations confirm quantitatively that α-amines are much less favored to forming Schiff base adducts than Lys ε-amino groups. At near-physiological pH and temperature, the apparent dissociation constant for Schiff base formation with A_2 ($K_d \approx 0.5$ M) is high, but much lower than for the Lys ε-amine ($K_d \approx 10$ M). We attribute this difference to the higher electronegativity of C^{α} compared to Lys C^{ε}, which also is responsible for the much lower pK_a value of α- compared to ε-amines.

Our work shows that ^{1}H-CEST NMR is remarkably sensitive to detection of even very small ($\leq 0.1\%$) fractions of transient reaction intermediates, and that adaptation of this CEST experiment can provide quantitative rate information over a very wide kinetic range. The more than 10-fold lower population of Schiff base adduct with Lys ε-amino groups compared to α-amines explains why the former is difficult to observe experimentally. Nevertheless, even the very small, transient population of Schiff base adduct with Lys ε-amines is sufficiently large to be trapped by reaction with free DOPAL, then forming the previously reported DCPL, capable of protein cross linking.

Acknowledgements

We thank J. L. Baber and J. Ying for technical support, and J. M. Courtney, T. Kakeshpour, R. L. Levine, A. J. Robertson, D. A. Torchia, and V. Tugarinov for valuable discussions. This work was supported by the Intramural Research Program of

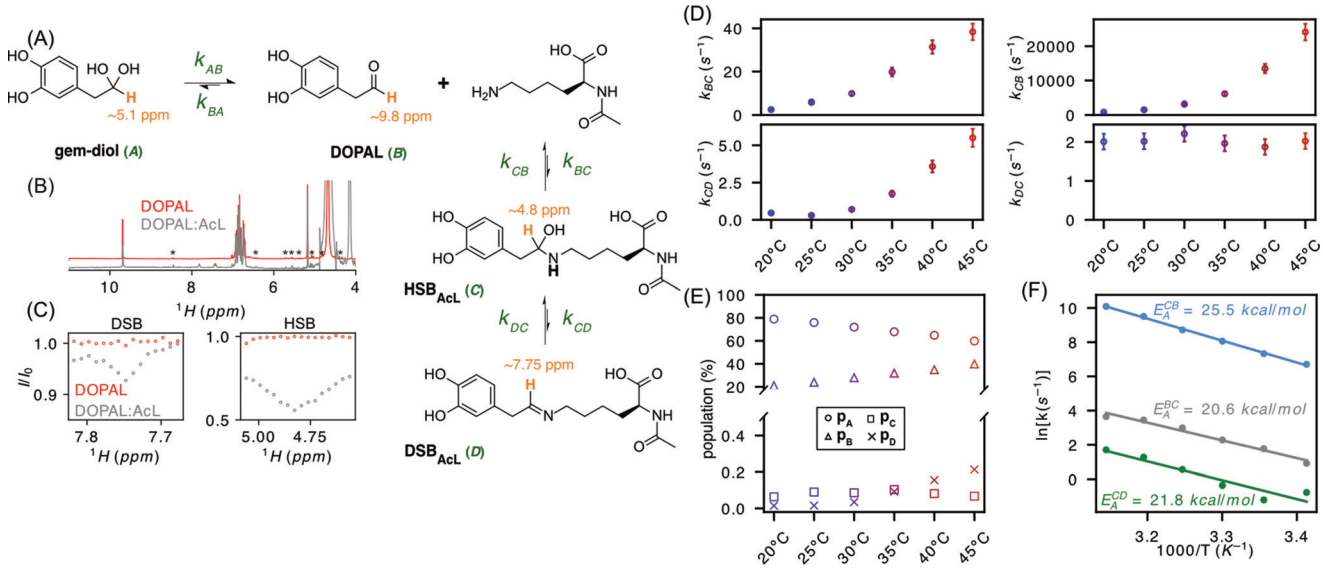

Figure 3. Schiff base formation between DOPAL and N$^{\alpha}$-acetyl lysine. A) Reaction Scheme. B) ^{1}H spectra of 2 mM DOPAL in the absence (red) and presence (gray) of 30 mM AcL. Asterisks correspond to impurities in our starting material. C) Zoomed region of ^{1}H-CEST on DSB (left) measured with $B_1 = 6$ Hz, $\tau_{CEST} = 15$ s at 40 °C and HSB (right) measured with $B_1 = 30$ Hz, $\tau_{CEST} = 5$ s at 20 °C. Both measurements were carried out on a 2 mM DOPAL sample in absence (red) and presence (gray) of 30 mM AcL. D) Rate constants fitted as a function of temperature: k_{BC} (top left), k_{CB} (top right), k_{CD} (top left), k_{DC} (top left). E) Populations derived from the rate constants as a function of temperature: pA (○), p_B (△), p_C (□), p_D (×). Uncertainties in these populations are estimated at ±0.3 % (p_A and p_B) and ±0.02 % (p_C and p_D). F) Activation energies calculated for the DOPAL/Schiff base reaction ($E_A^{BC} = 20.6 \pm 1.6$ kcal mol^{-1} and $E_A^{CB} = 25.5 \pm 0.5$ kcal mol^{-1}) and the hemiaminal/Schiff base reaction ($E_A^{CD} = 21.8 \pm 3$ kcal mol^{-1}). k_{DC} has no significant temperature dependence, and E_A^{DC} was smaller than 3 kcal mol^{-1}.

the National Institute of Diabetes and Digestive and Kidney Diseases.

Conflict of interest

The authors declare no conflict of interest.

Keywords: CEST NMR Spectroscopy · DOPAL · reaction intermediates · Schiff base · synuclein

How to cite: *Angew. Chem. Int. Ed.* **2019**, *58*, 15309–15312
Angew. Chem. **2019**, *131*, 15453–15456

[1] H. Schiff, *Ann. Chem. Pharm.* **1864**, *131*, 118–119.
[2] M. Chan-Huot, S. Sharif, P. M. Tolstoy, M. D. Toney, H. H. Limbach, *Biochemistry* **2010**, *49*, 10818–10830.
[3] S. Sharif, G. S. Denisov, M. D. Toney, H. H. Limbach, *J. Am. Chem. Soc.* **2006**, *128*, 3375–3387.
[4] J. W. Werner-Allen, J. F. DuMond, R. L. Levine, A. Bax, *Angew. Chem. Int. Ed.* **2016**, *55*, 7374–7378; *Angew. Chem.* **2016**, *128*, 7500–7504.
[5] J. W. Werner-Allen, S. Monti, J. F. DuMond, R. L. Levine, A. Bax, *Biochemistry* **2018**, *57*, 1462–1474.
[6] H. Blaschko, *Pharmacol. Rev.* **1952**, *4*, 415–458.
[7] W. M. Panneton, V. B. Kumar, Q. Gan, W. J. Burke, J. E. Galvin, *PLoS One* **2010**, *5*, e15251.
[8] D. S. Goldstein, I. J. Kopin, Y. Sharabi, *Pharmacol. Ther.* **2014**, *144*, 268–282.
[9] E. Monzani, S. Nicolis, S. Dell'Acqua, A. Capucciati, C. Bacchella, F. A. Zucca, E. V. Mosharov, D. Sulzer, L. Zecca, L. Casella, *Angew. Chem. Int. Ed.* **2019**, *58*, 6512–6527; *Angew. Chem.* **2019**, *131*, 6580–6596.
[10] N. Plotegher, G. Berti, E. Ferrari, I. Tessari, M. Zanetti, L. Lunelli, E. Greggio, M. Bisaglia, M. Veronesi, S. Girotto, M. Dalla Serra, C. Perego, L. Casella, L. Bubacco, *Sci. Rep.* **2017**, *7*, 40699.
[11] J. N. Rees, V. R. Florang, L. L. Eckert, J. A. Doorn, *Chem. Res. Toxicol.* **2009**, *22*, 1256–1263.
[12] C. Follmer, E. Coelho-Cerqueira, D. Y. Yatabe-Franco, G. D. T. Araujo, A. S. Pinheiro, G. B. Domont, D. Eliezer, *J. Biol. Chem.* **2015**, *290*, 27660–27679.
[13] P. Vallurupalli, G. Bouvignies, L. E. Kay, *J. Am. Chem. Soc.* **2012**, *134*, 8148–8161.
[14] C. Gladkova, A. F. Schubert, J. L. Wagstaff, J. N. Pruneda, S. M. V. Freund, D. Komander, *EMBO J.* **2017**, *36*, 3555–3572.
[15] A. L. Hansen, L. E. Kay, *Proc. Natl. Acad. Sci. USA* **2014**, *111*, E1705–E1712.
[16] C. Lorenz, F. Hastreiter, J. Hioe, N. Lokesh, S. Gartner, N. Korber, R. M. Gschwind, *Angew. Chem. Int. Ed.* **2018**, *57*, 12956–12960; *Angew. Chem.* **2018**, *130*, 13138–13142.
[17] N. Lokesh, A. Seegerer, J. Hioe, R. M. Gschwind, *J. Am. Chem. Soc.* **2018**, *140*, 1855–1862.
[18] S. Forsén, R. A. Hoffman, *J. Chem. Phys.* **1963**, *39*, 2892–2901.
[19] K. M. Ward, A. H. Aletras, R. S. Balaban, *J. Magn. Reson.* **2000**, *143*, 79–87.
[20] P. C. M. van Zijl, N. N. Yadav, *Magn. Reson. Med.* **2011**, *65*, 927–948.
[21] Y. Jinsmaa, V. R. Florang, J. N. Rees, L. M. Mexas, L. L. Eckert, E. M. G. Allen, D. G. Anderson, J. A. Doorn, *Chem.-Biol. Interact.* **2011**, *192*, 118–121.
[22] V. Amarnath, D. C. Anthony, K. Amarnath, W. M. Valentine, L. A. Wetterau, D. G. Graham, *J. Org. Chem.* **1991**, *56*, 6924–6931.
[23] A. Kornienko, J. J. La Clair, *Nat. Prod. Rep.* **2017**, *34*, 1051–1060.

Manuscript received: July 7, 2019
Accepted manuscript online: August 26, 2019
Version of record online: September 17, 2019

